Nuclear spin precession in ultra low fields - a probe for physics beyond the standard model

Lutz Trahms

Physikalisch-Technische Bundesanstalt

Outline

1. Low magnetic fields and what they are good for
2. Probing the low energy range by nuclear spin precession
3. Searching Axions

Low magnetic fields

1. Low magnetic fields and what they are good for
2. Probing the low energy range by nuclear spin precession
3. Searching Axions

Berlin Magnetically Shielded Room - 2

- Passive magnetic shielding
  7-layers of mu-metal
- One eddy-current layer
- Active shielding coil system
  (feedback control)
- Shielding performance @ 0.1Hz

  Passive shielding: $2{\cdot}10^5$
  With active shielding: $2{\cdot}10^7$

BMSR-2 – a walkable room
3 x 3 x 3 m^3

Low magnetic fields

Berlin Magnetically Shielded Room - 2

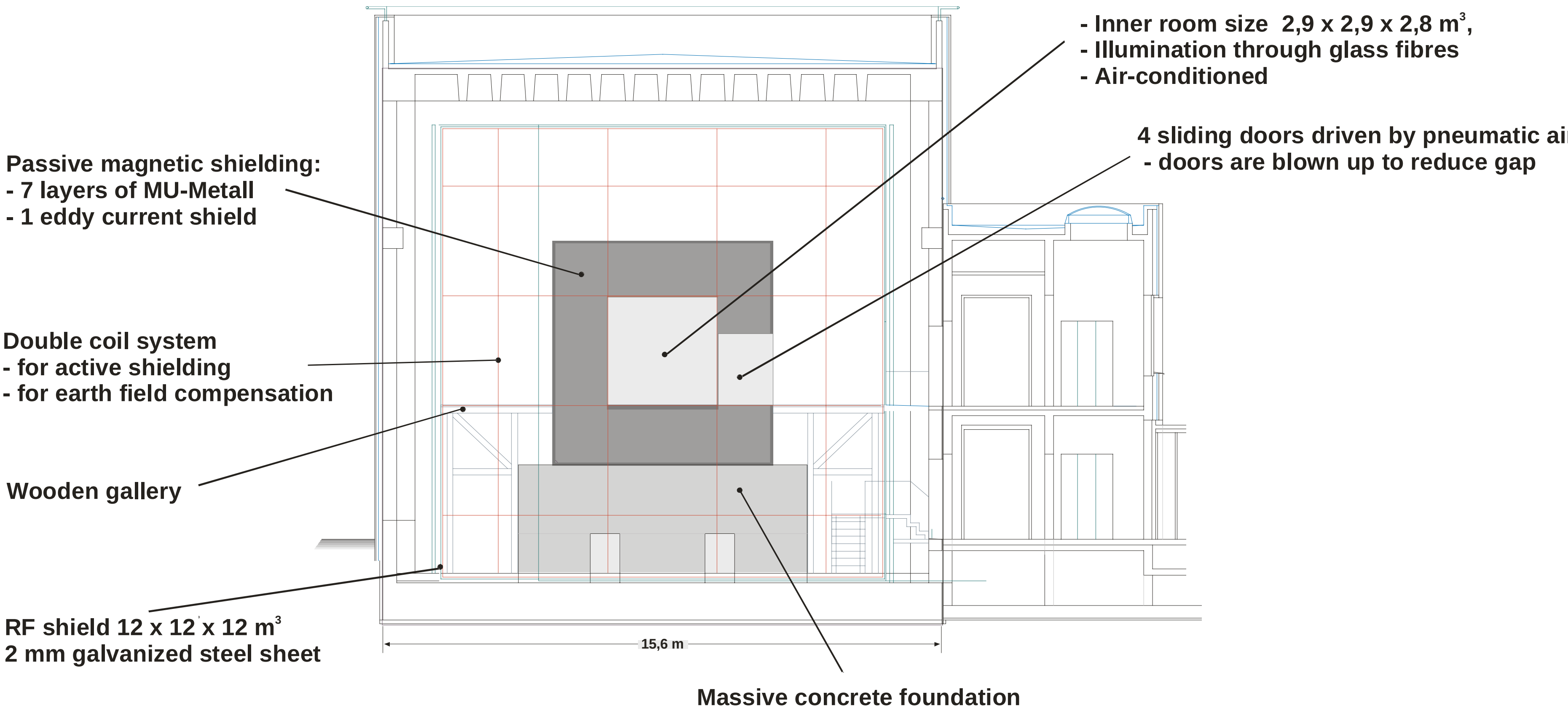

Berlin Magnetically Shielded Room - 2

Residual static field < 200 pT

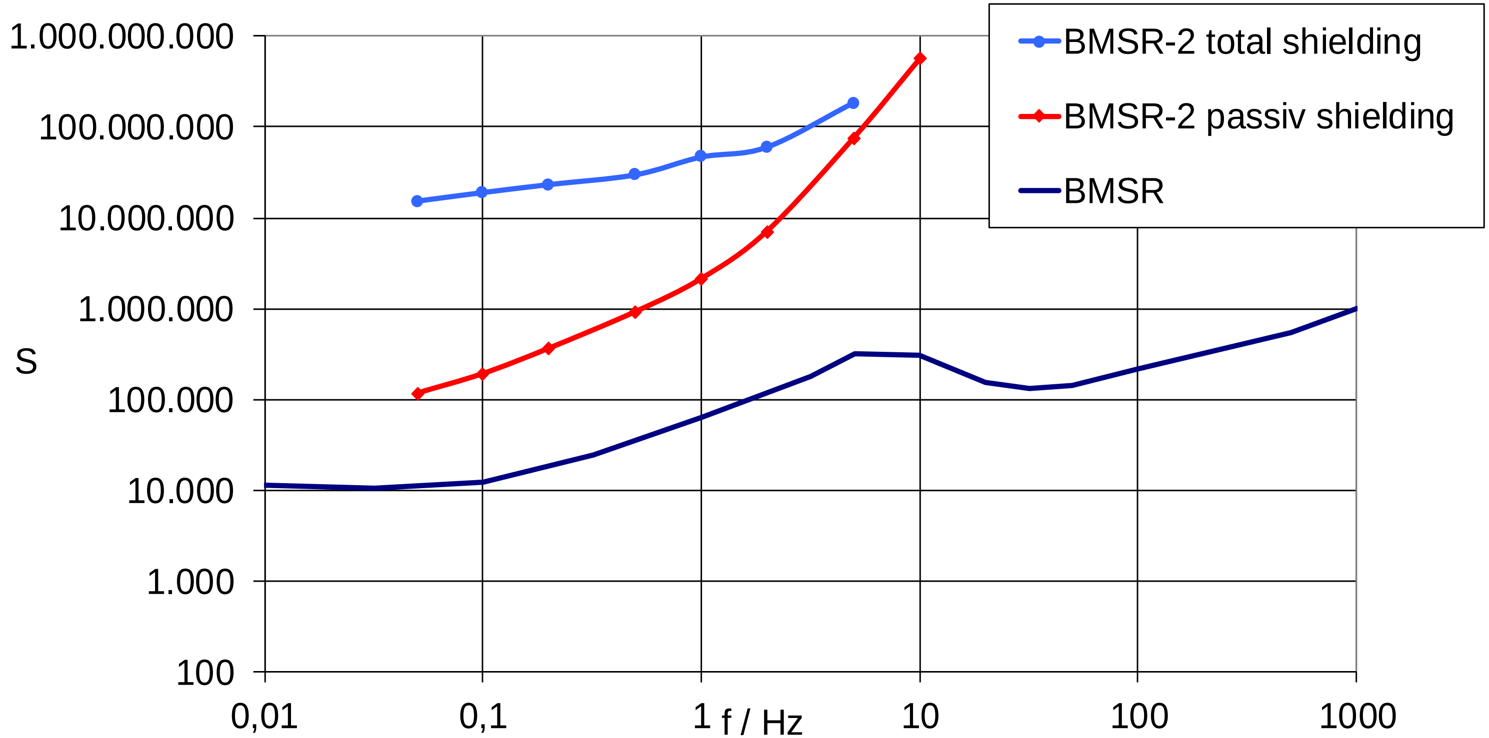

Shielding factor vs. frequency

Low magnetic fields

Superconducting Quantum Interference Device

liquid He
Dewar

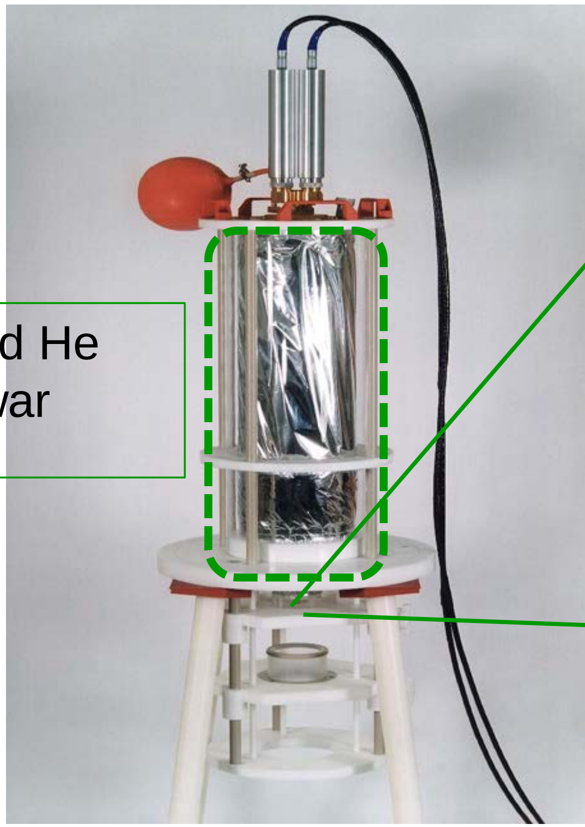

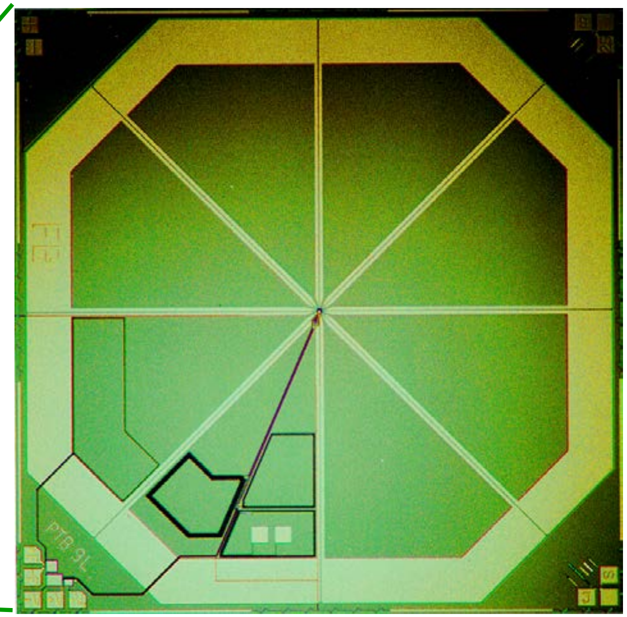

7 mm

„Cart-wheel“ design
by D. Drung

Low magnetic fields

Noise spectrum of the SQUIDs in the 304 channel device

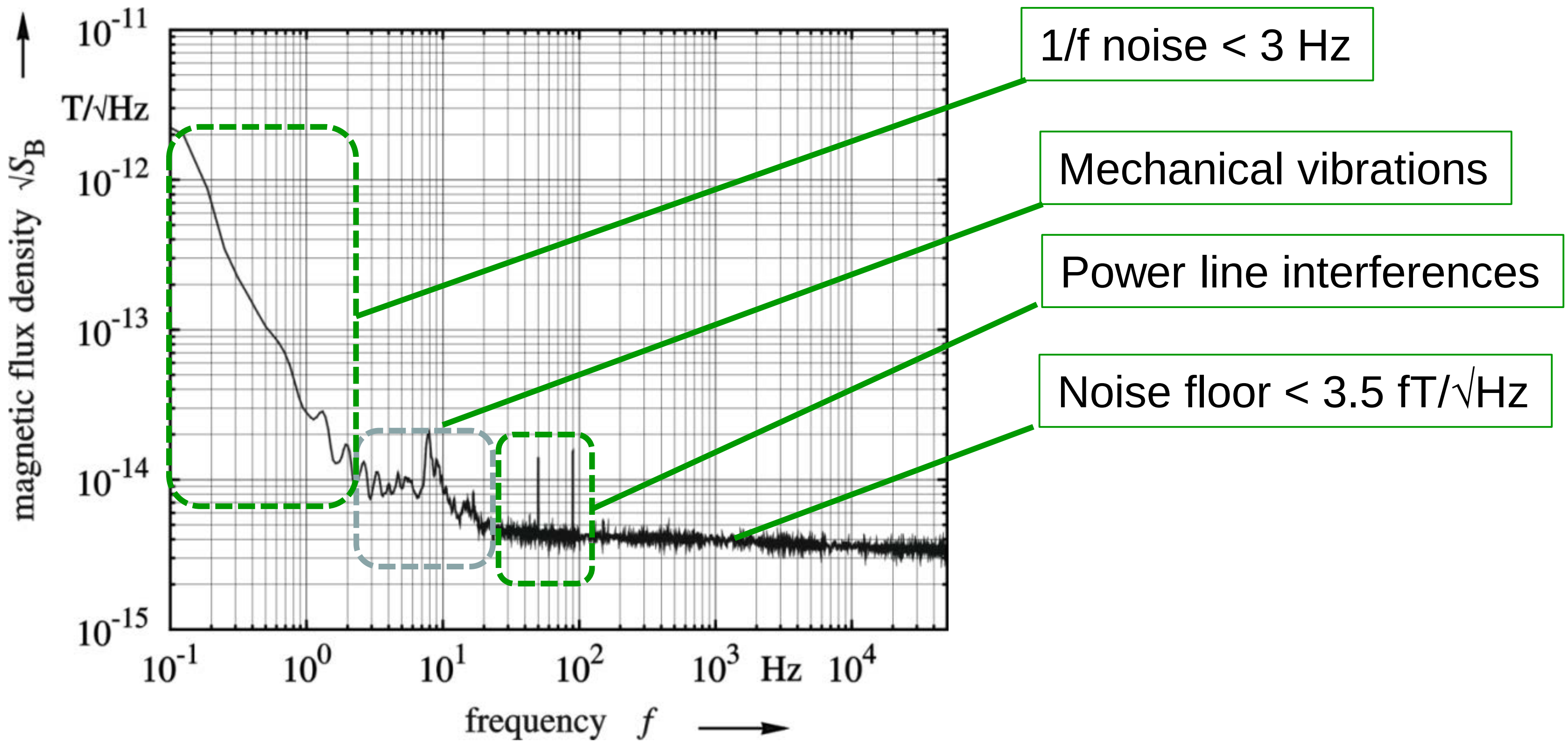

D. Drung
High-performance DC SQUID
read-out electronics
Physica C 368 (2002) 134-140

Applications :MCG

Magnetocardiography

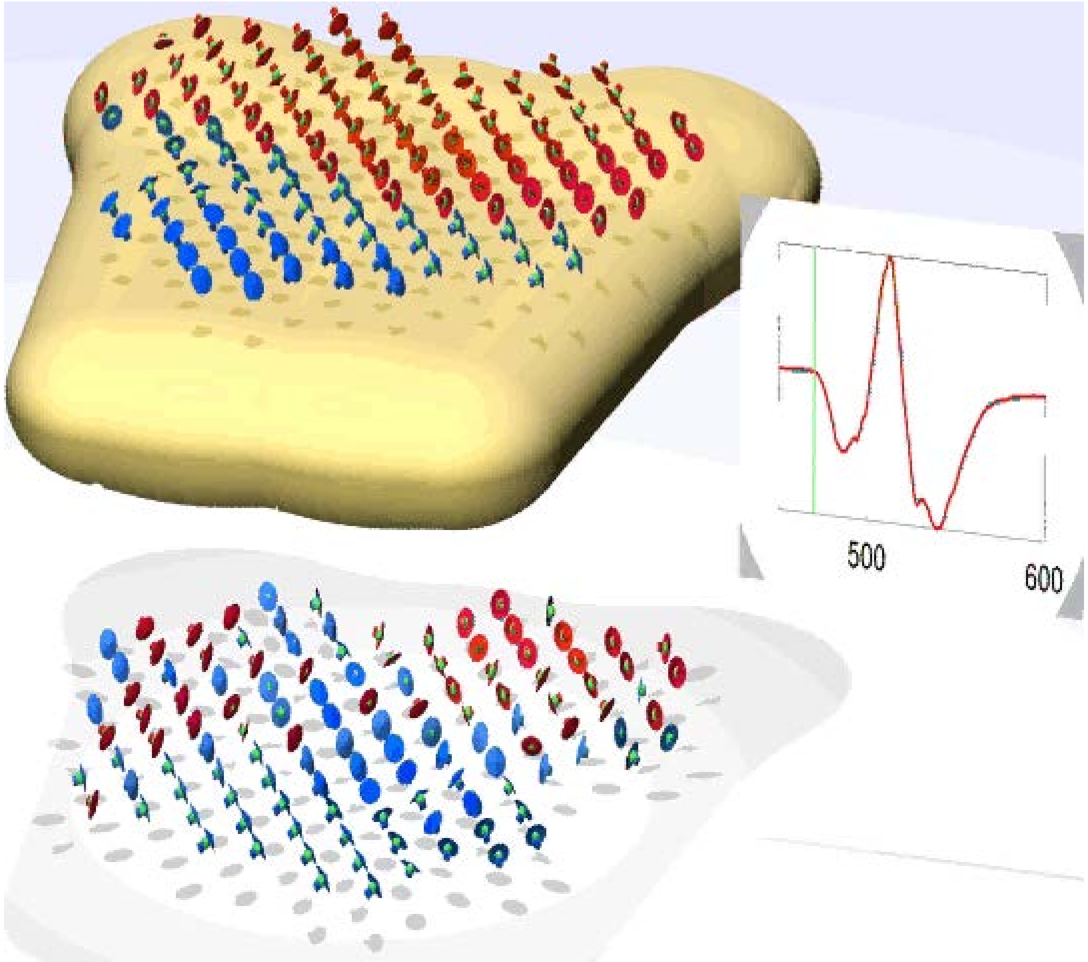

- more information content
- reduced uncertainty
- better reconstruction of current density

Brockmeier et al. (1997) J Cardiovasc Electrophysiol

Applications: MEG

Multichannel
SQUID device

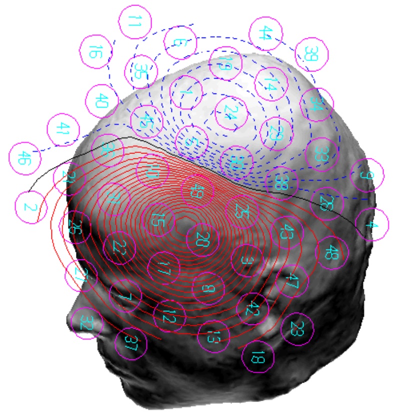

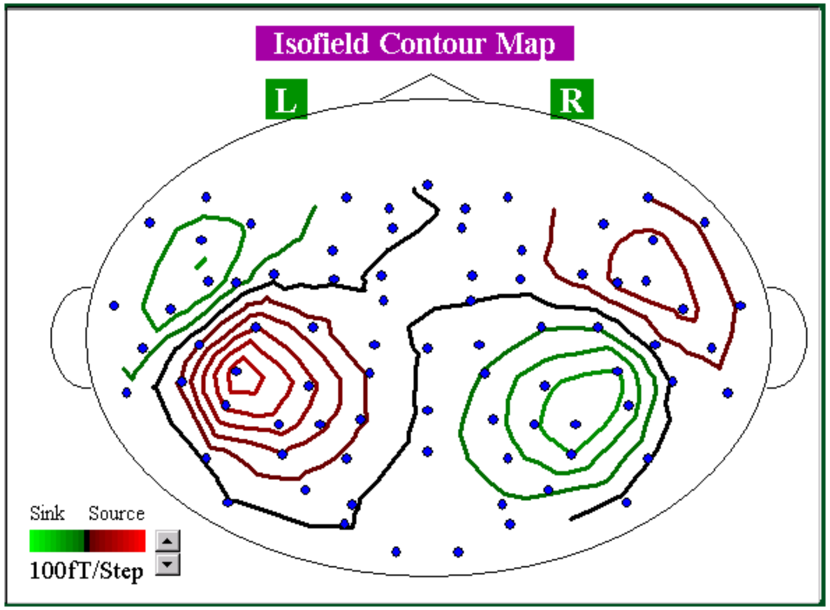

Brain's magnetic response after
auditory simulation

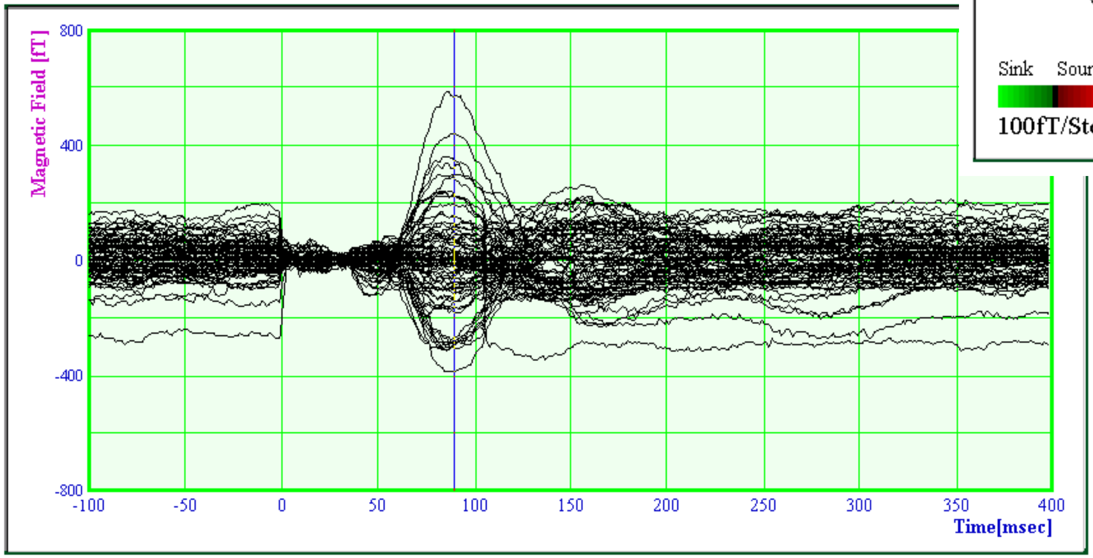

Isocontour plot of the
evoked magnetic field
90 ms after stimulation

Salajegheh et al (2004) Neuroimage

Applications: MEG

Magnetoencephalography

Localization of the current source in the brain

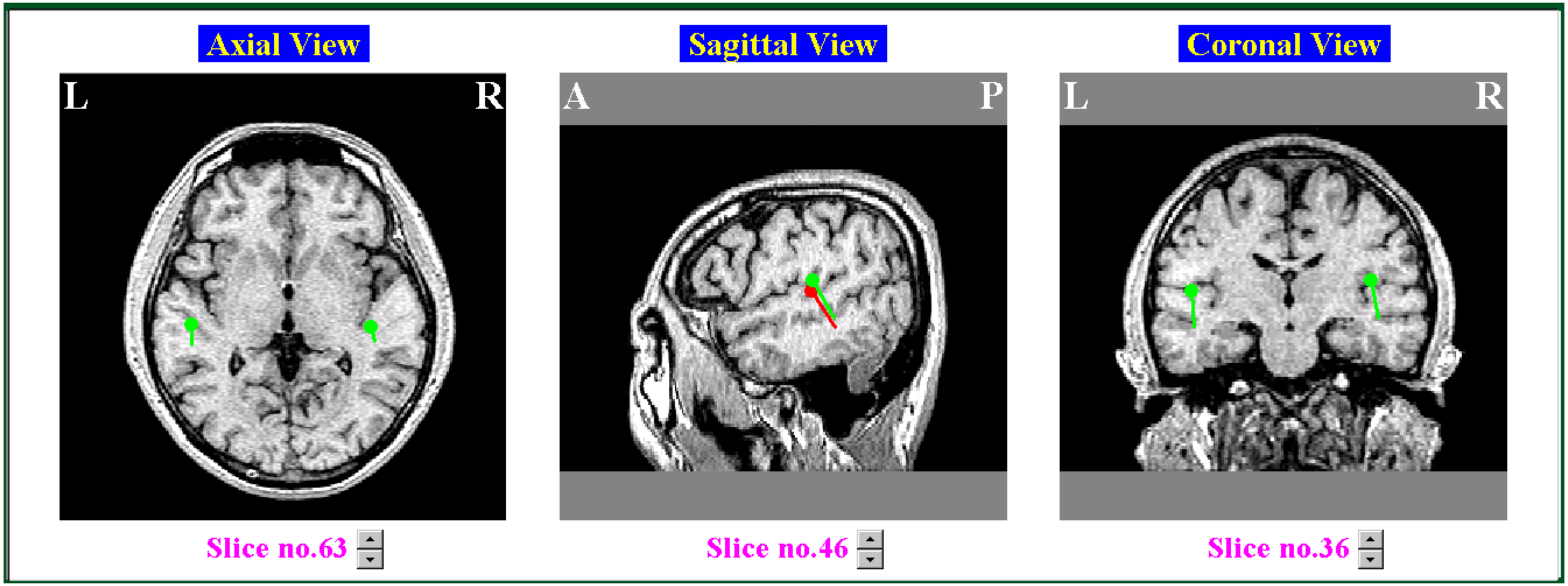

Applications: MNG

Magnetoneurogram

Propagation of the action potential
in the tibial nerve

Patient with a conduction block
in the right leg

Functional localization of the block

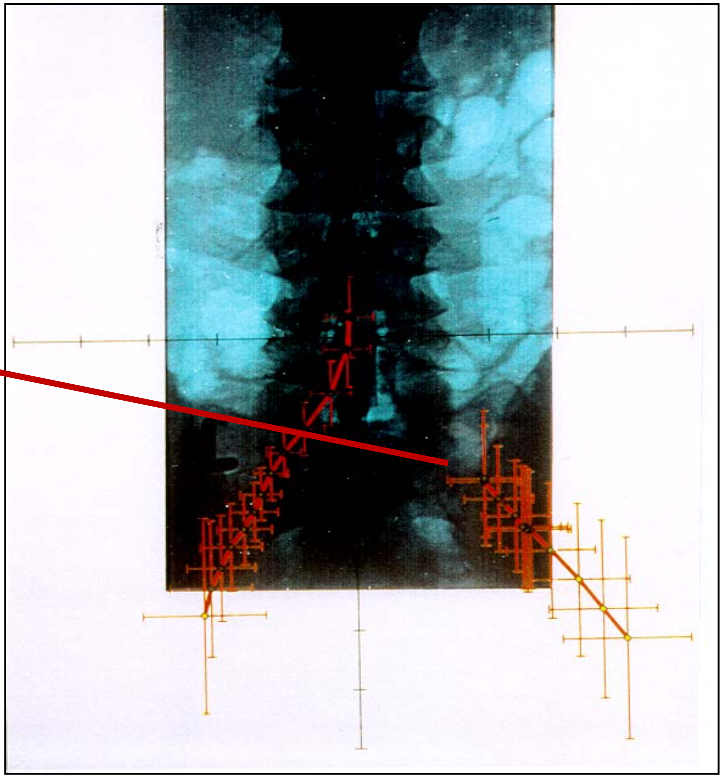

Mackert et al (1998) Electroenceph Clin Neurophysiol

Magnetic nanoparticles for cancer therapy

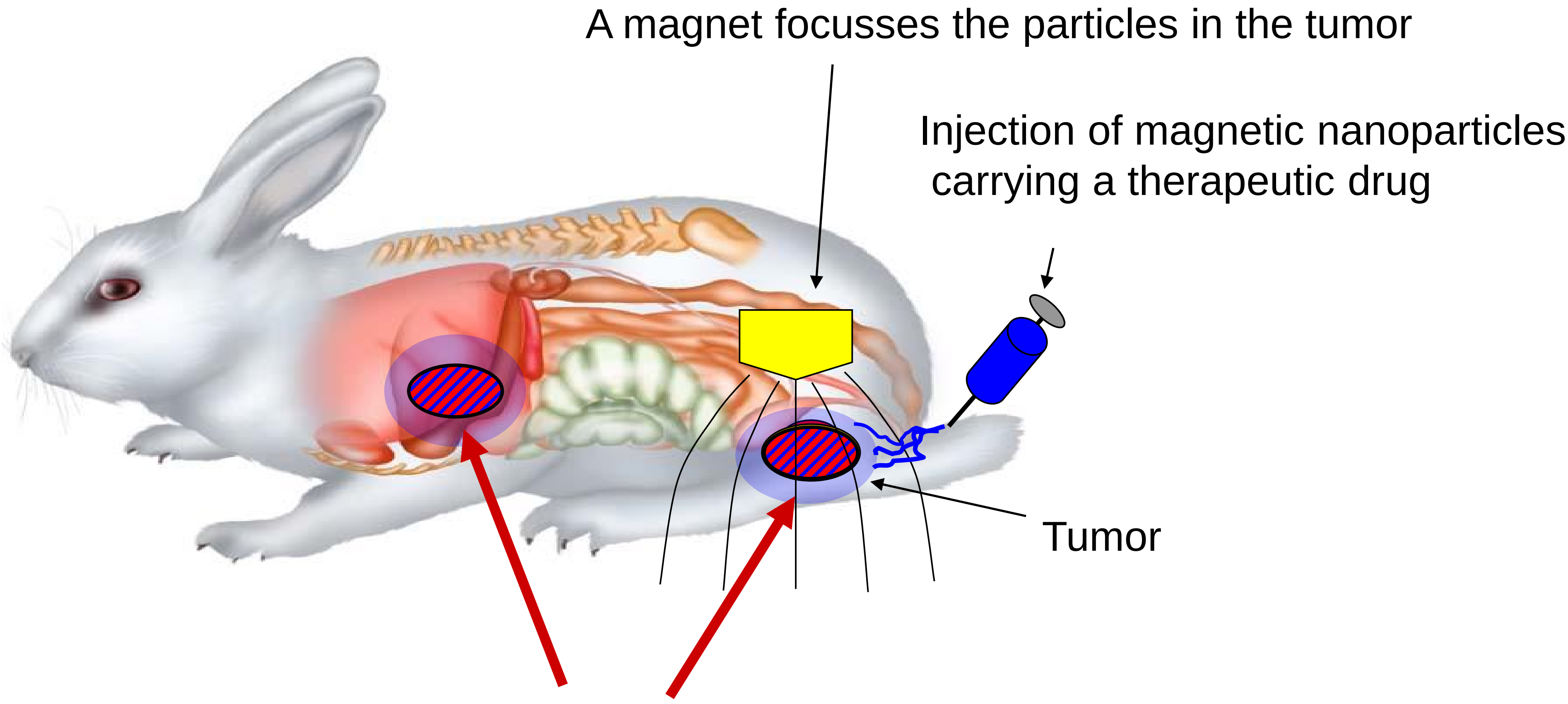

What is the biodistribution of the MNP ?

Applications: MNP

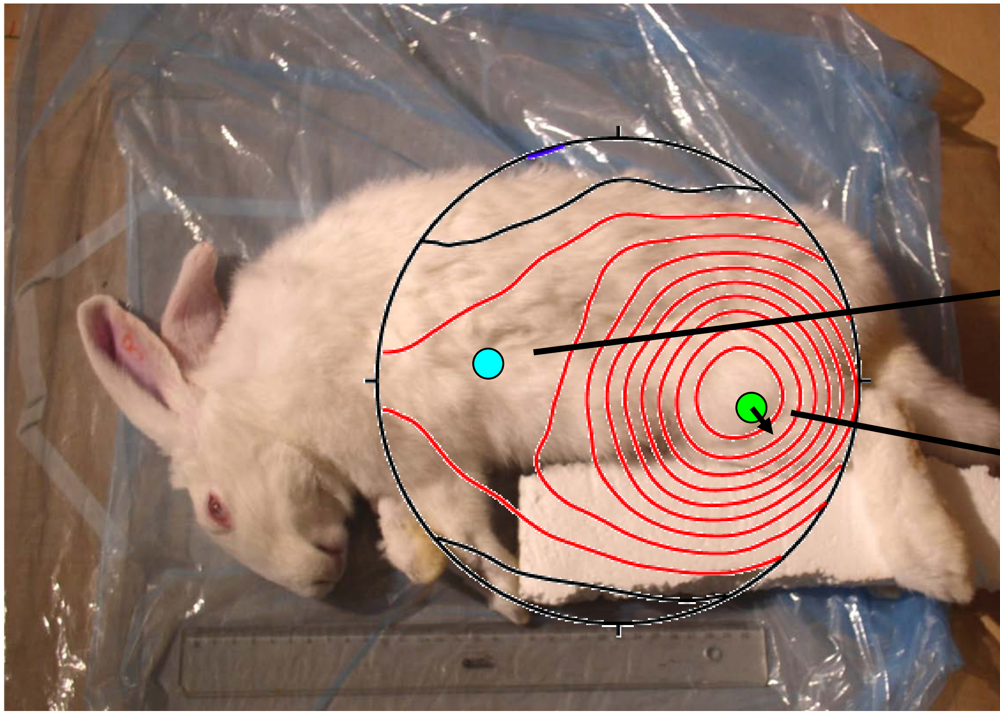

Magnetic field distribution reflects two sources

Source reconstruction is quantitative,
but spatial resolution is limited

Wiekhorst et al (2012) Pharmaceut Res

Applications: NMR

^{1}H NMR: Relaxation in water revisited

$T_{1,2}$-relaxation rates at different Larmor frequencies
(fields between 100 nT and 50 mT)

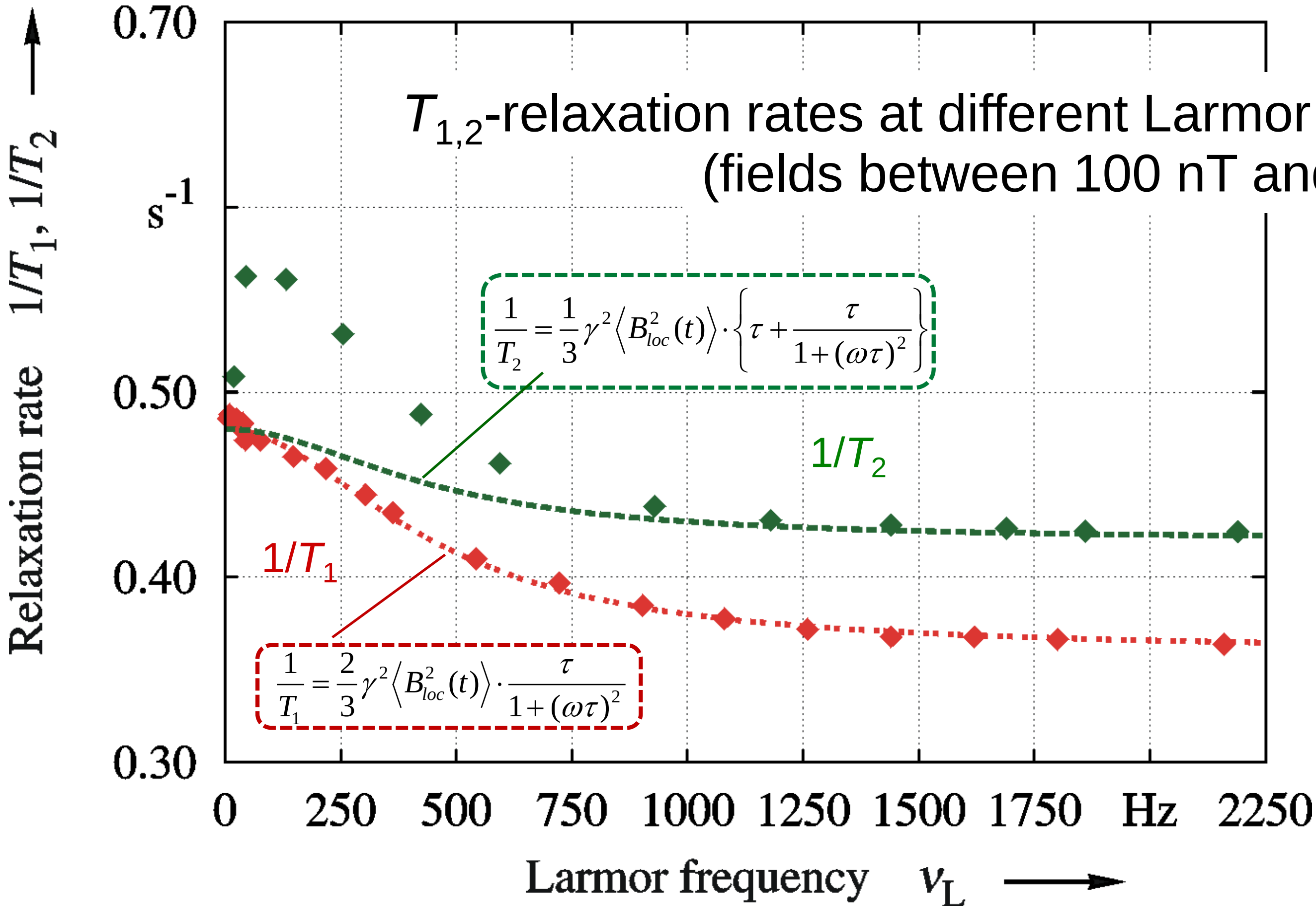

Hartwig et al (2011) J Chem Phys

Nuclear spin precession

1. Low magnetic fields and what they are good for

2. Probing the low energy range by nuclear spin precession

3. Searching Axions

Nuclear spin precession

Helmholtz-Coils inside BMSR-2

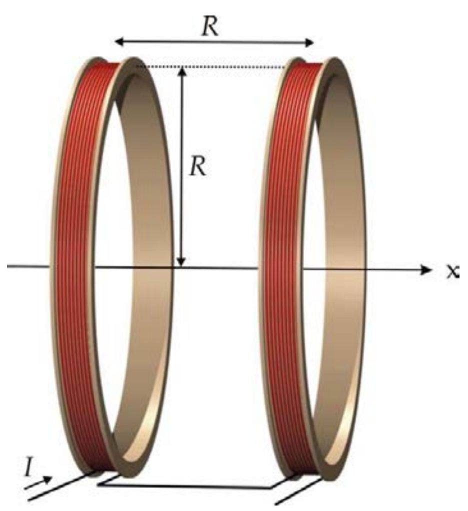

+

$B_0 = \sim 1\mu\text{T}$
Homogeneity across sample volume : $\Delta B_0 = \sim 100$ pT

$B_{\text{res}} = \sim 200$ pT
Homogeneity across sample volume : $\Delta B_{\text{res}} = \sim 10$ pT

Nuclear spin precession

3D Helmholtz-Coils inside BMSR-2

Dewar
filled with liquid He

SQUID

Glass bulb
filled with
hyperpolarized ^{3}He
and/or ^{129}Xe

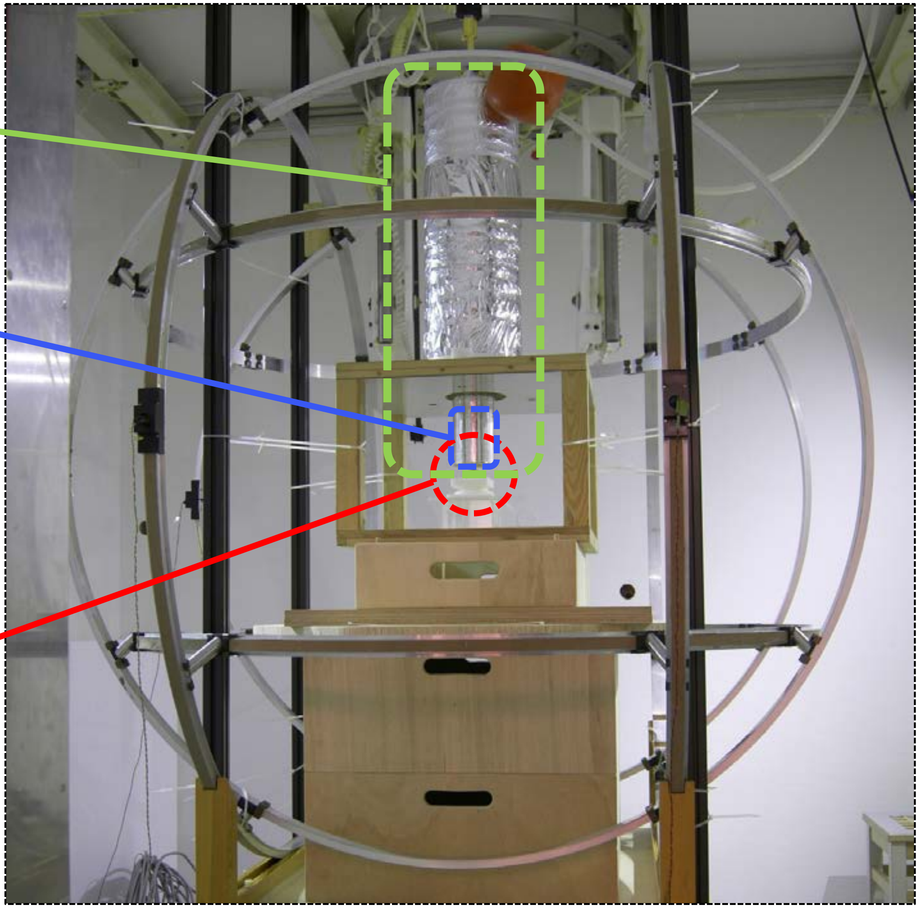

Generation of nuclear magnetization

Hyperpolarized ^{3}He and ^{129}Xe by optical pumping (10%-30%)

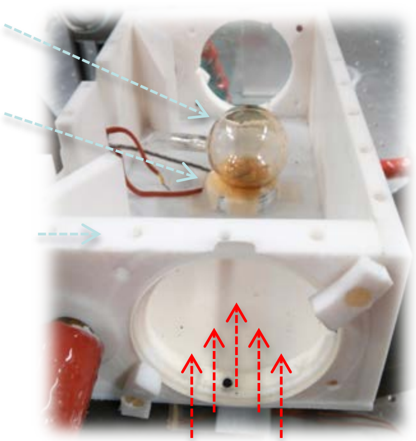

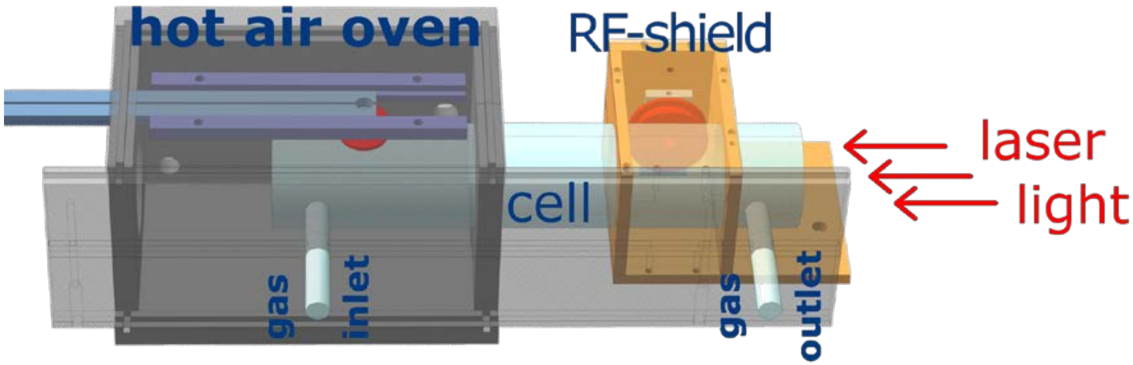

B_{He} = 10 pT … 30 pT

W. Kilian

Nuclear spin precession

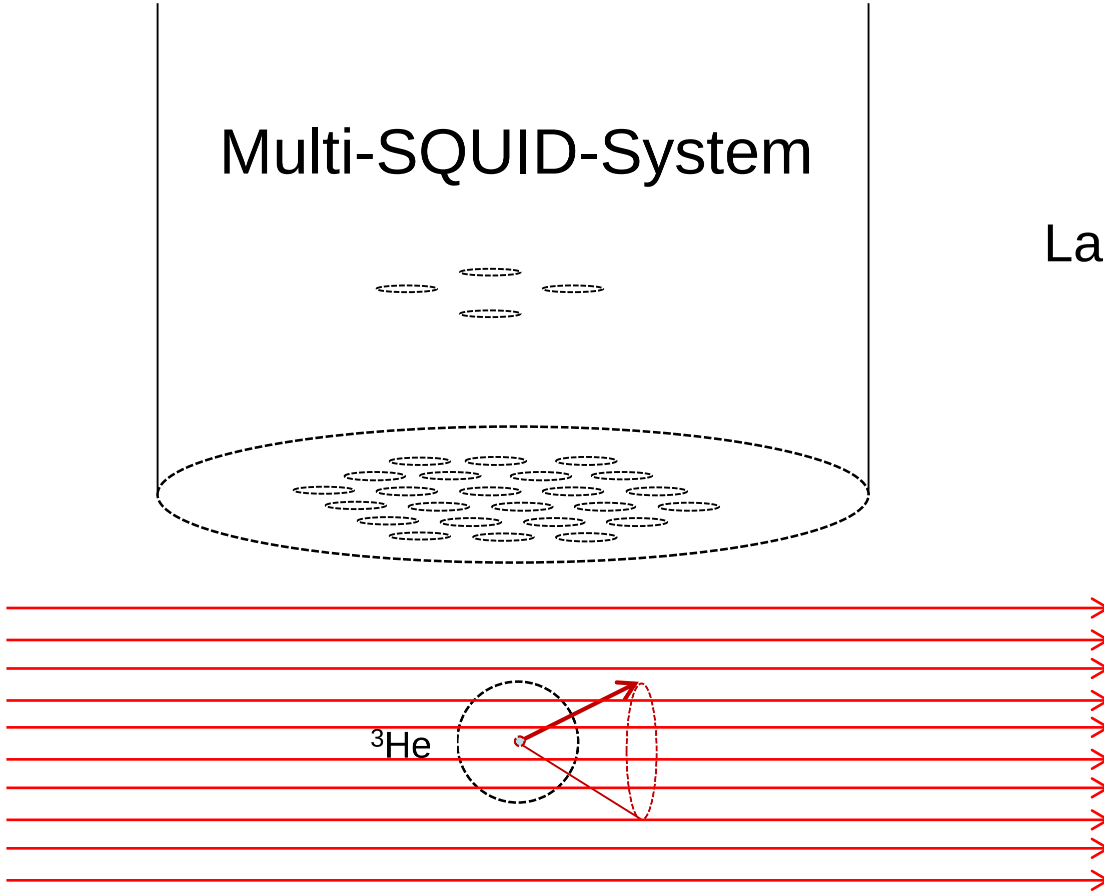

B_0

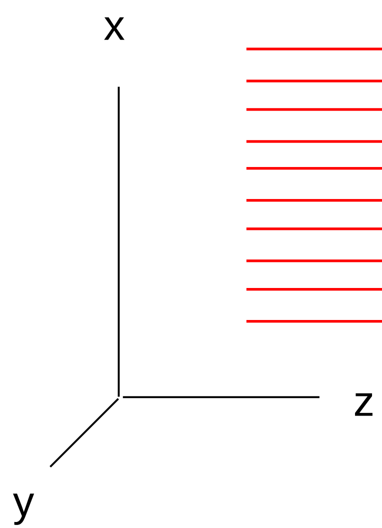

Larmor precession

$$\omega = \gamma B_0$$

$$m_x(t) = m_\perp^0 e^{-t/T_2^*} \cos \omega t$$
$$m_y(t) = m_\perp^0 e^{-t/T_2^*} \sin \omega t$$
$$m_z(t) = m_z^0 e^{-t/T_1}$$

Nuclear spin precession

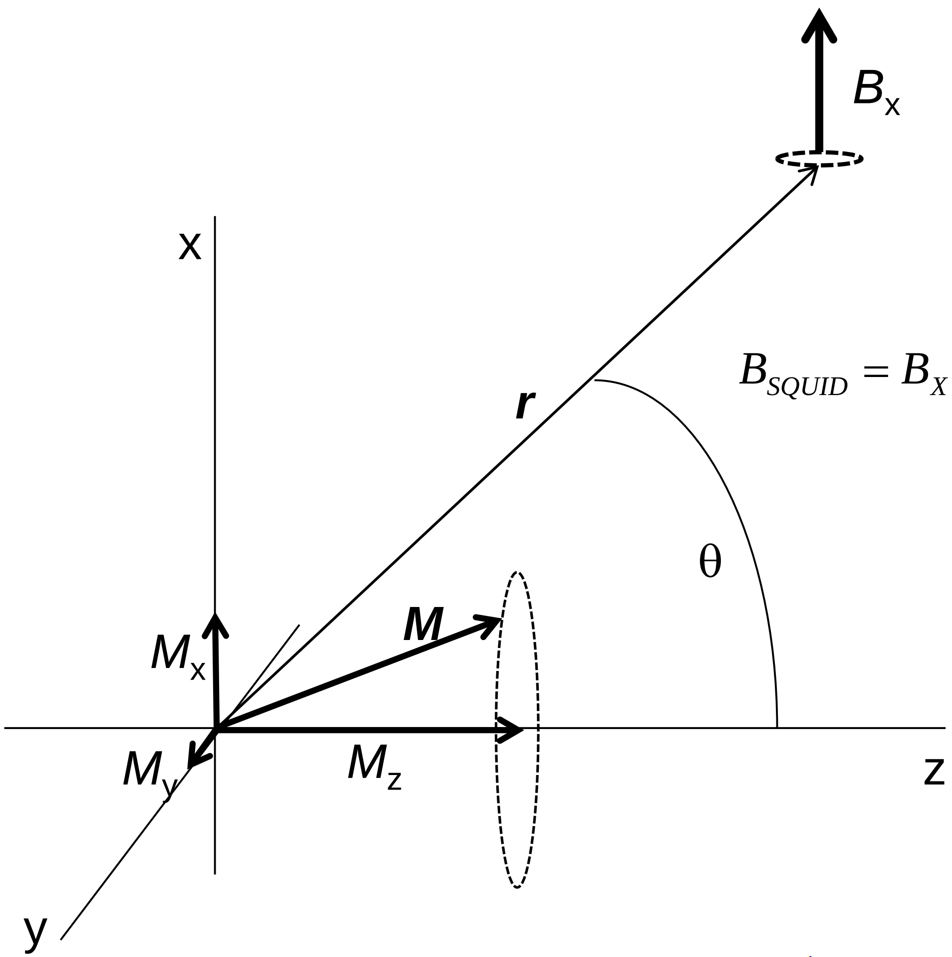

Signal seen by SQUID:

$$B_{SQUID} = B_X(t) = \frac{\mu_0}{4\pi \cdot |\vec{r}|^3} \cdot \left(\frac{3x^3 m_X(t)\vec{e}_X}{|\vec{r}|^2} - m_X(t)\vec{e}_X \right)$$

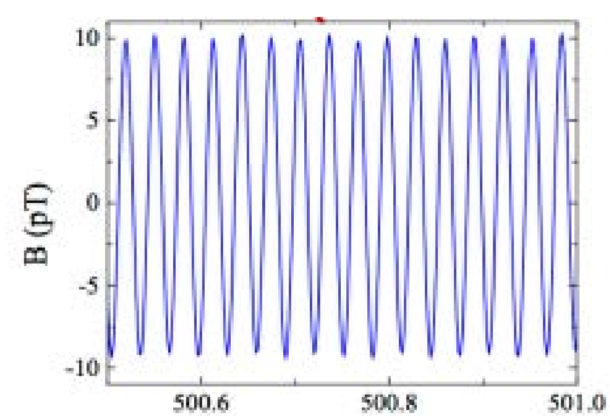

$$m_x(t) = m_\perp^0 e^{-t/T_2^*} \cos \omega t$$
$$m_y(t) = m_\perp^0 e^{-t/T_2^*} \sin \omega t$$
$$m_z(t) = m_z^0 e^{-t/T_1}$$

Nuclear spin precession

Example: ^{3}He spin

Amplitude of the sinusodial signal over time:

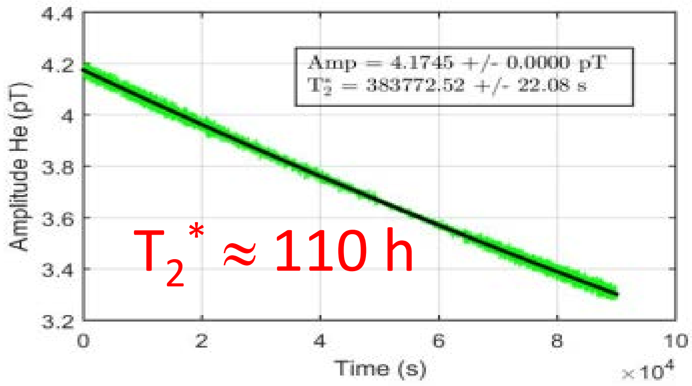

Magnetic spectral flux density:

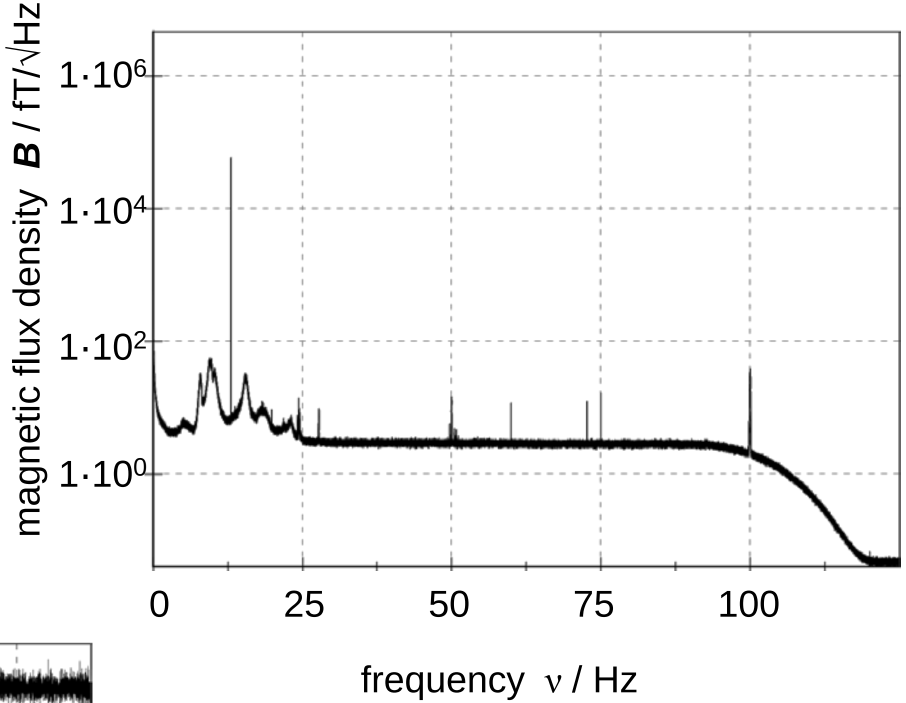

Lamor frequency over time:

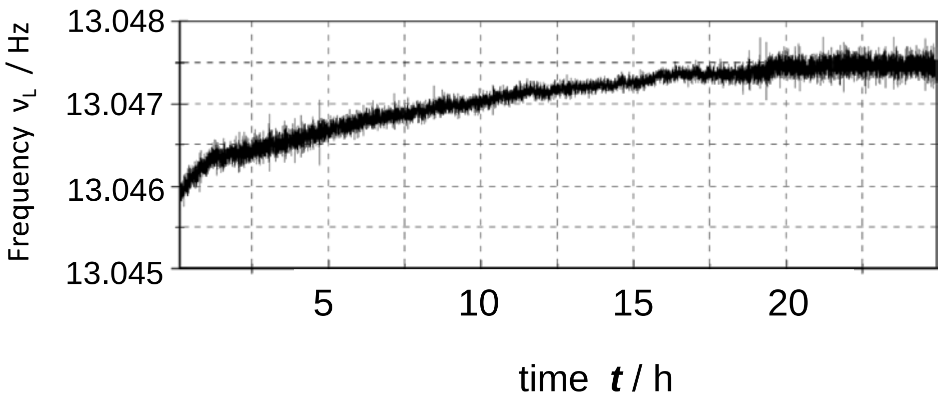

Nuclear spin precession

Transverse relaxation rate $$\frac{1}{T_2^*} = \Gamma_{\mathrm{Grad}} + \Gamma_{\mathrm{intr}}$$

$$\Gamma_{\mathrm{grad}} = \frac{4R^4\gamma^2}{175D}\left(|\nabla B_y|^2 + |\nabla B_z|^2 + 2|\nabla B_x|^2\right)$$

Low fields $\Longrightarrow$ small gradients $\Longrightarrow$ long T_2^*

Cates et al (1988) Phys Rev A

Limit of frequency resolution

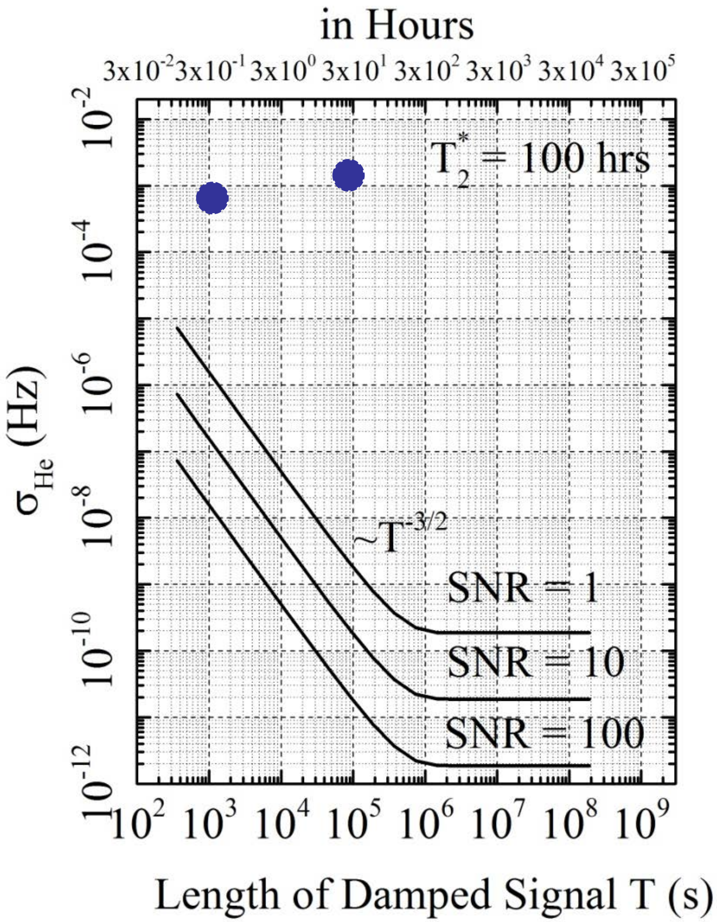

Theory:

Cramer-Rao lower bound for a decaying signal in the presence of white noise

$$\sigma_\nu \geq \frac{\sqrt{3}}{\pi \cdot SNR \cdot \sqrt{\nu_{BW} \cdot T^3}} \cdot \sqrt{C(T, T_2^*)}$$

$$\left.\begin{array}{l} T_2^* = 100\text{ h} \\ \nu_{BW} = 0.3\text{ Hz} \\ SNR = 100 \\ C(T, T_2^*) \sim 1 \end{array}\right\} \longrightarrow \begin{array}{l} \sigma \sim 5 \times 10^{-11}\text{ Hz} \\ \Delta E \sim 2 \times 10^{-25}\text{ eV} \end{array}$$

Slow field drifts spoil the resolution

Nuclear spin precession

Increase frequency stability by:

- Two gas species in one bulb, e.g. HeXe comagnetometer
  weighted frequency difference is independed of B_0 drifts

$$\Delta\omega = \omega_{He} - \frac{\gamma_{He}}{\gamma_{Xe}}\omega_{Xe} = 0$$

- gas/SQUID comagnetometer: measure B_0 drift with an independent SQUID and build a B_0 locked loop (i.e. B_0LL) or use results for offline correction

Axion search

1. Low magnetic fields and what they are good for
2. Probing the low energy range by nuclear spin precession
3. Searching Axions

Axion search

Axion like particles (ALPs):

- act on the nucleus like an alternating magnetic field *
- modulation of the precession frequency
- Unknown frequency ν_{ALP} ~ mass m_{ALP}
- Axion coherence time $10^{-6}/\nu_{ALP}$

* P. Graham and S. Rajendran, PRD 2011, 2013

Introducing:

Axion-o-meter

based on frequency change
of free precessing noble gas nuclei

Axion search

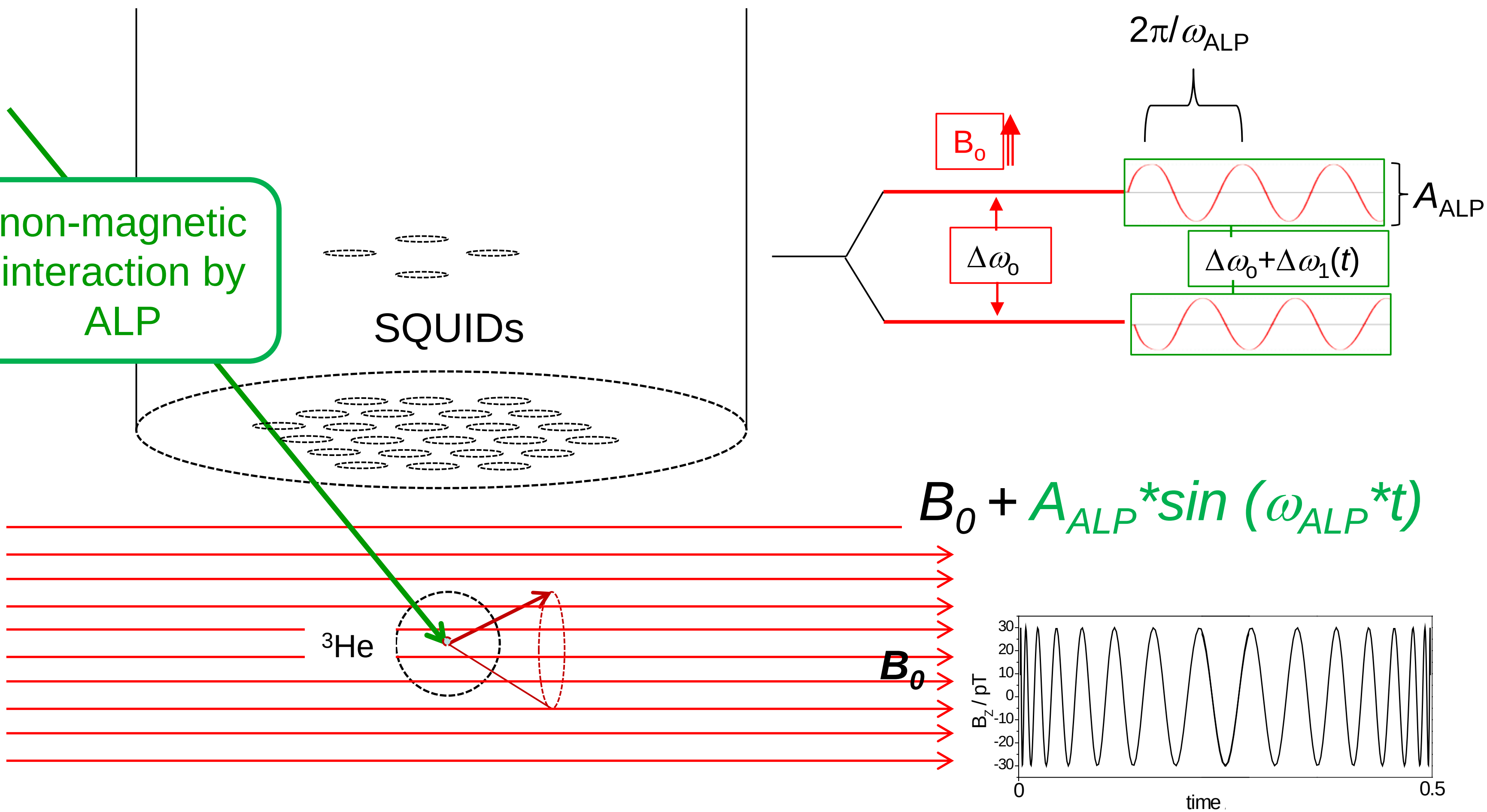

P. Graham and S. Rajendran, PRD 2011, 2013

Axion search

Frequency modulation

$$\omega_L = \gamma B \Longrightarrow \omega(t) = \omega_L + I \sin(\omega_{ALP} t)$$

Signal measured by the SQUID:

$$B_{SQUID}(t) = B_{He} * \sin\left(\omega_L + I \sin(\omega_{ALP}\, t)\right) * t$$

with modulation index $I = \dfrac{\gamma * A_{ALP}}{\omega_{ALP}}$

Axion search

Sinusodial change of B_0 ⟹ frequency modulation of ω_L

results in sidebands at $\omega_L \pm \omega_{ALP}$:

a) $\omega_{ALP} < \omega_L$

b) $\omega_{ALP} > \omega_L$

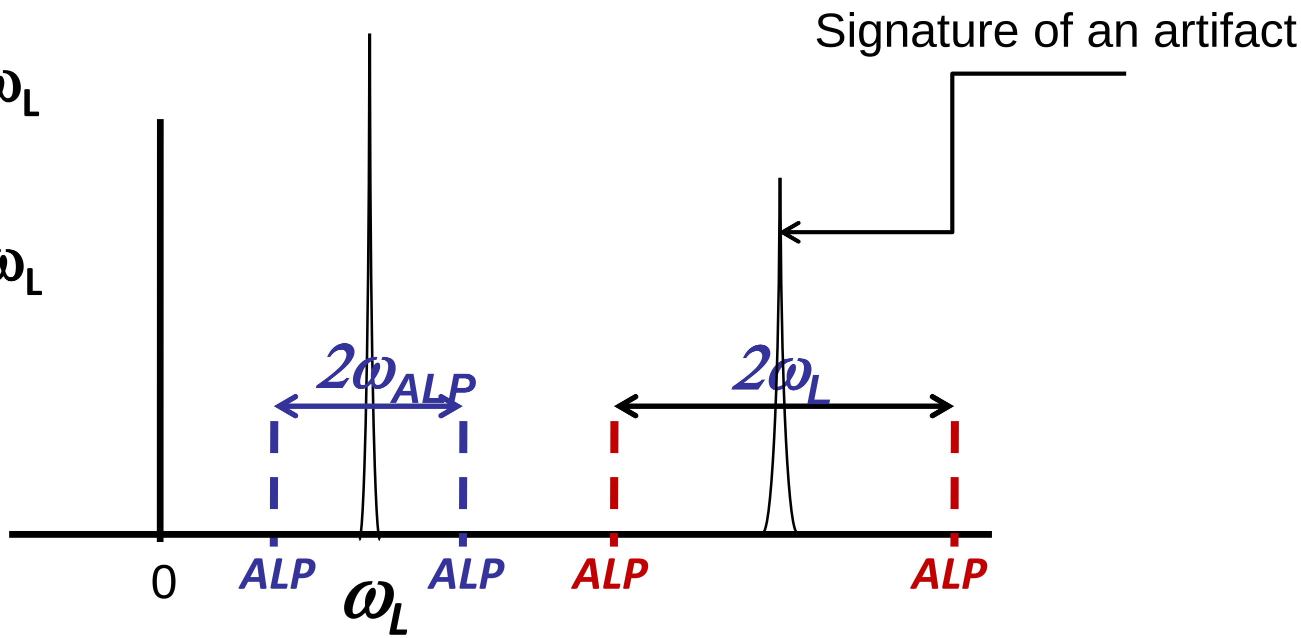

Axion search

The amplitude of the side band is given by the Bessel function

$$J_n(I) = \sum_{s=1}^{\infty} \frac{(-1)^s}{s!(n+s)!} \left(\frac{I}{s}\right)^{n+2s} = \frac{I^n}{2^n n!} - \frac{I^{n+2}}{2^{n+2}(n+1)!} + \ldots$$

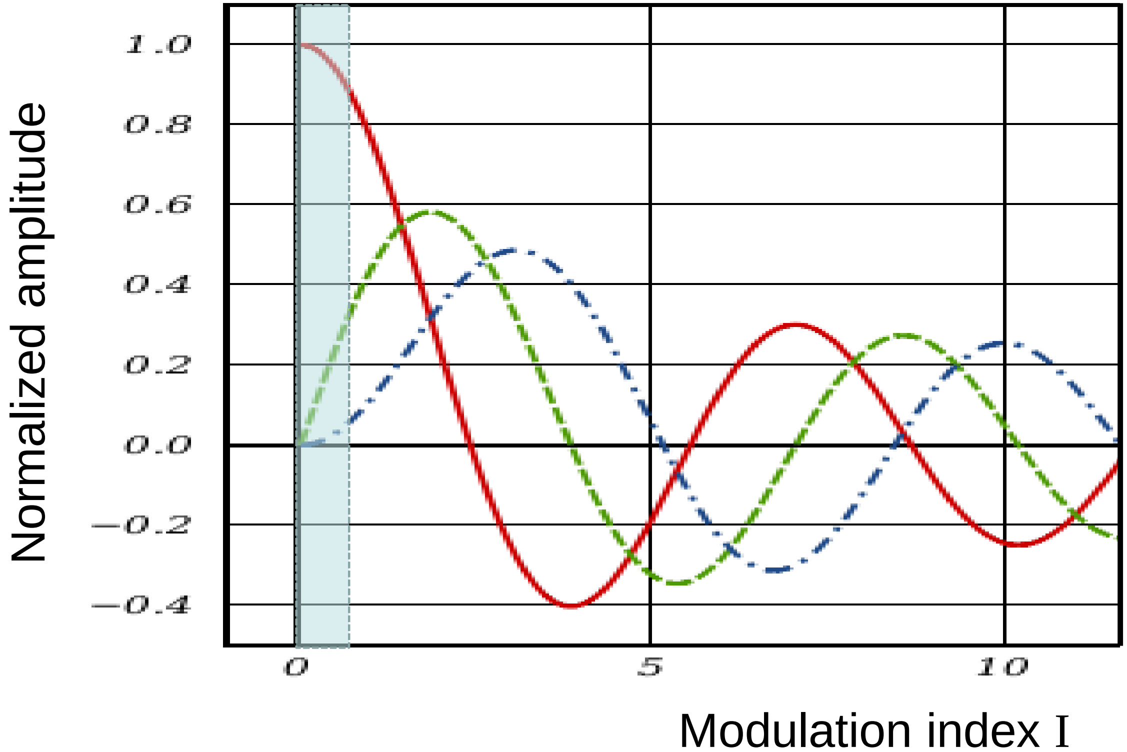

Sidebands:
- -- J_0 (carrier B_L)
- -- J_1
- -- J_2

Choose constraints:

$$0.5 > I = \frac{\gamma * A_{ALP}}{\omega_{ALP}}$$

Axion search : Demo

Demonstration of ALP detection principle

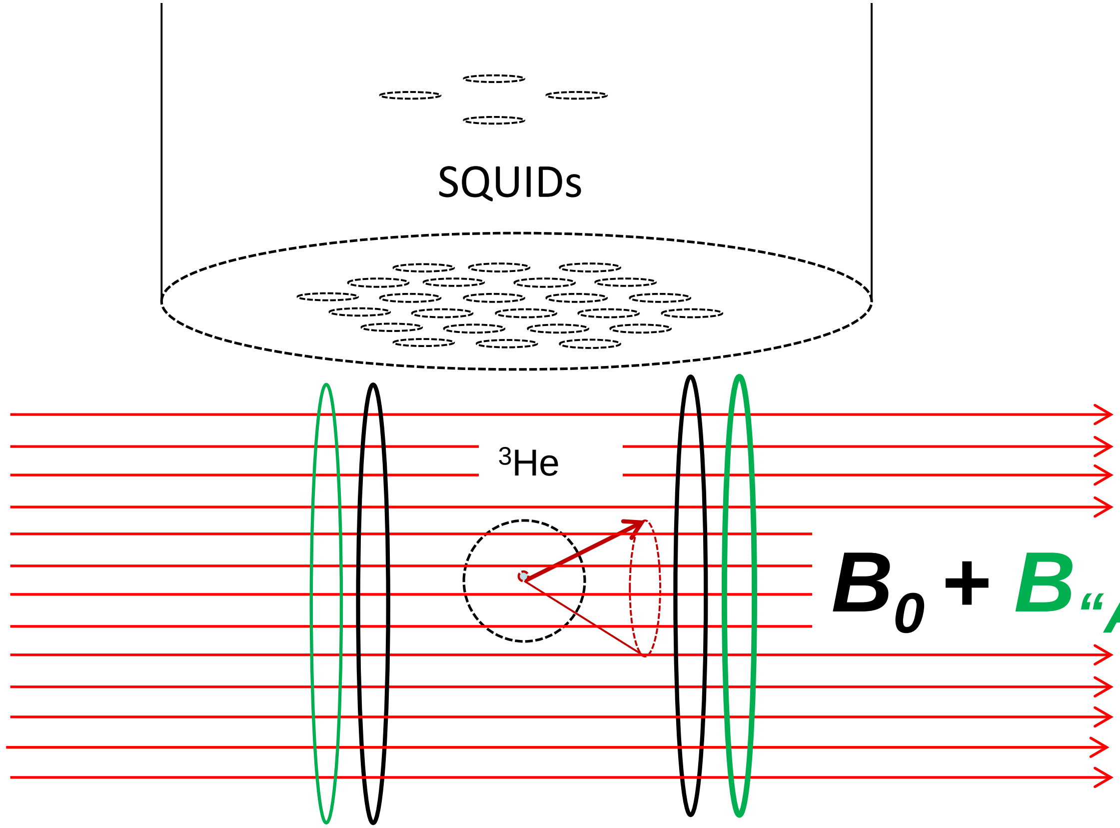

$$\boldsymbol{B_0 + B_{\text{“ALP“}} * \sin(\omega_{mod} * t)}$$

Feed a sinusodial current to a second Helmholz coil to produce a modulation field

Axion search : Demo

Apply a modulation by HH coil:

$B_{“ALP“} = 1$ nT

$\nu_{“ALP“} = 1.5$ Hz

Experimental result:

$B_{HE} = 12.6$ fT

$B_{SB} = 0.145$ fT

Samples = 166586

(duration 11 min, ν_s=250 Hz)

Calculated result using

$\gamma_{He} = 32.434$ Hz/µT :

$B_{“ALP“} \approx \nu_{“ALP“} * 2 * B_{SB} / (\gamma * B_{He})$

$B_{“ALP“} = 1$ nT

Noise spectrum (amplitude density):

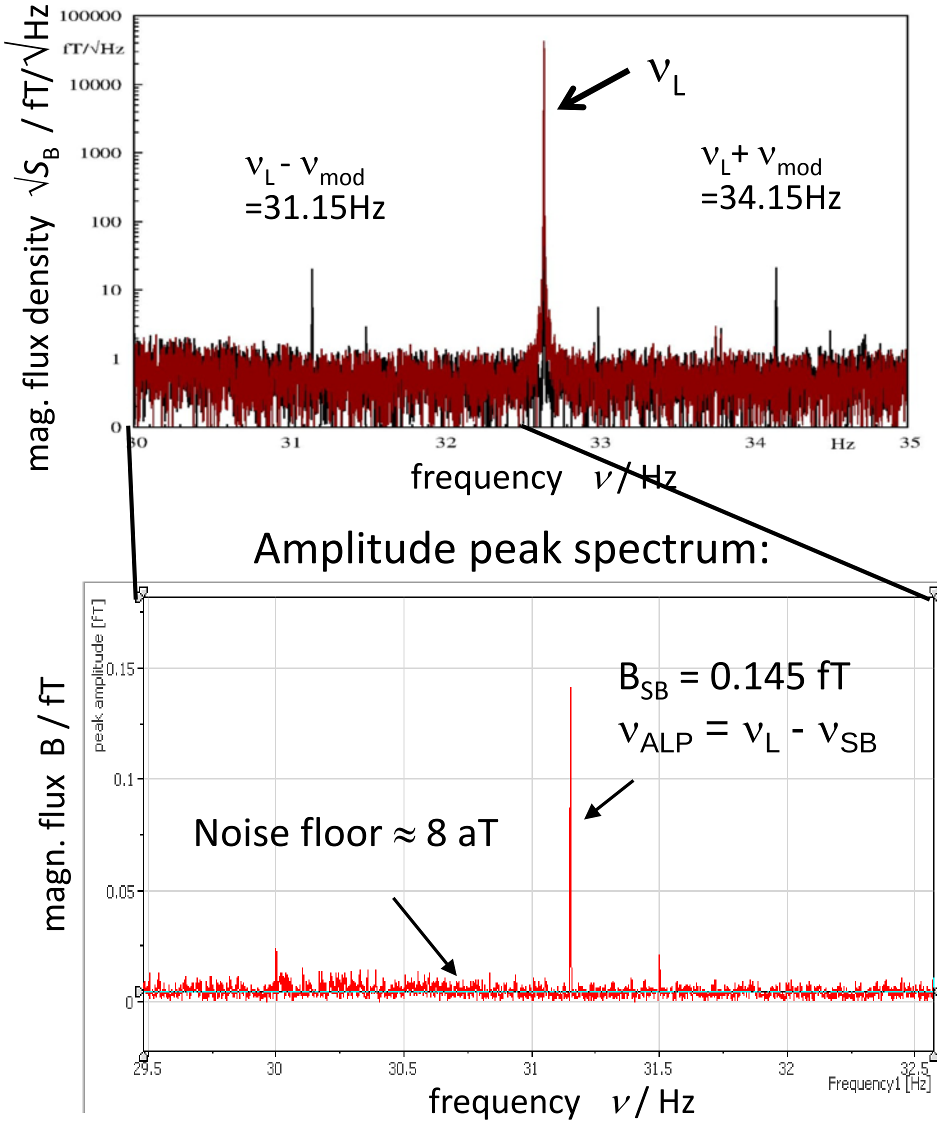

Limit of detection

Amplitude peak spectrum:

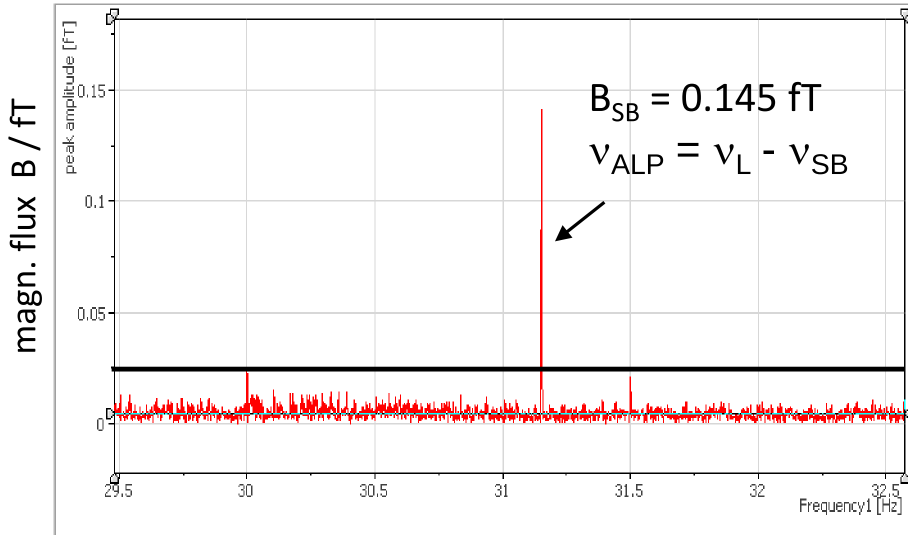

Noise floor (rms) = 7.3 aT ± 3.9 aT(k=1)

Limit of detection for one peak ~ 20 aT

Axion search

Limit of detection: Contourplot pseudo magnetic field B_{ALP} / fT

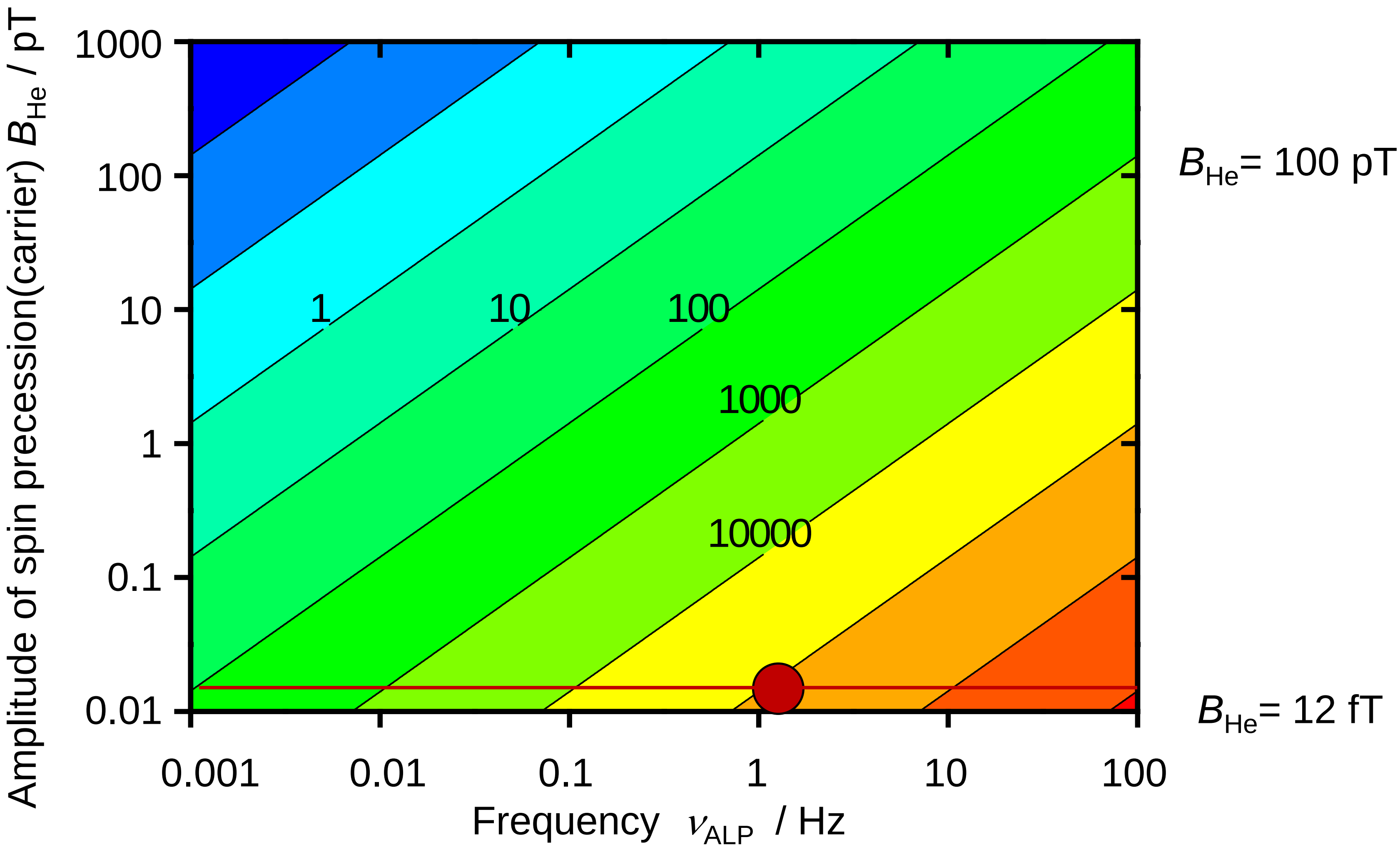

Axion search

Relation between axion wind coupling g_{aNN} and $B_{\text{“ALP“}}$:

$$g_{aNN} = \frac{\gamma_{He}}{2vm_a a} B_{"ALP"}$$

$$\Rightarrow \quad g_{aNN} = 3.1 \times 10^7 \left(\frac{B_{"ALP"}}{\mathrm{T}}\right) \mathrm{GeV}^{-1}$$

ν_{ALP}=0.01 Hz : $B_{\text{“ALP“}}$ = 100 aT
g_{aNN} = 3.1 x 10^{-9} GeV^{-1}

ν_{ALP}=10 Hz : $B_{\text{“ALP“}}$ = 100 fT
g_{aNN} = 3.1 x 10^{-6} GeV^{-1}

P. Graham

Axion search

Noise floor depends on number of samples N:

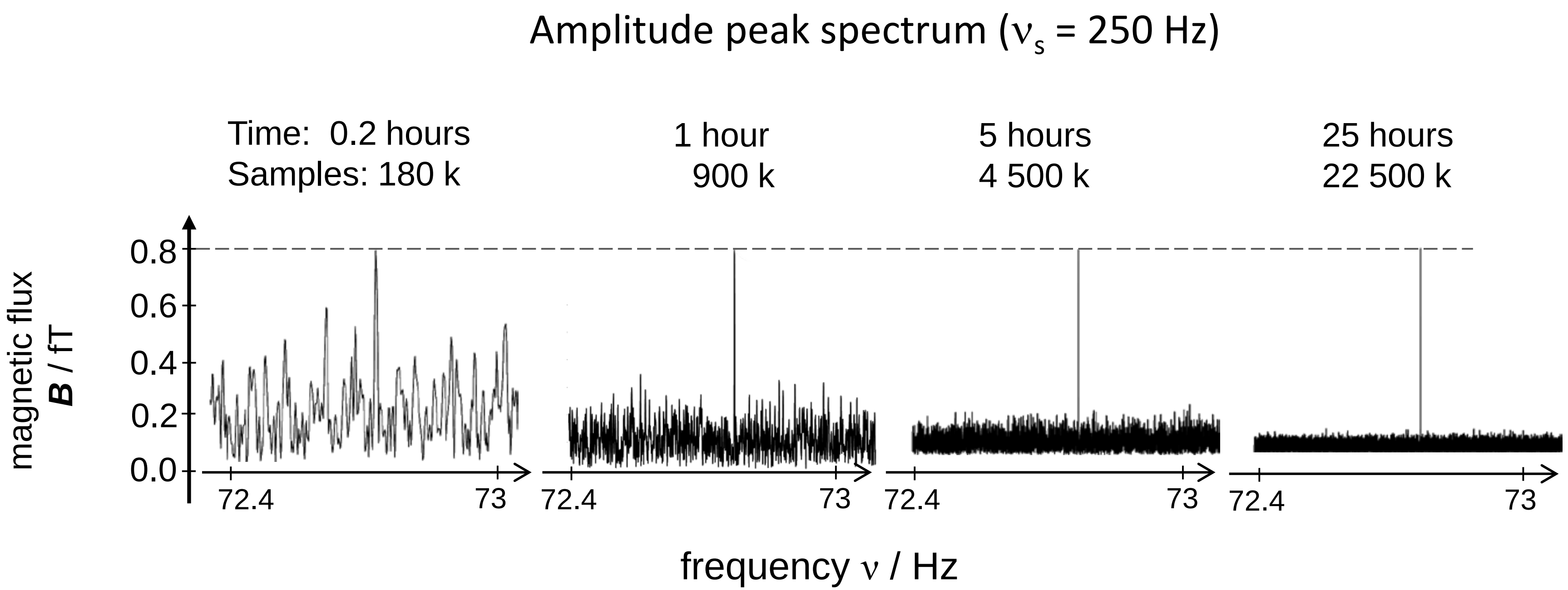

Noise floor ≈ 10V/18 bit - 10*log(N/2)

How long should we measure? → Axion coherence time?

→ earth rotation?

Conclusion

- Nuclear spin precession of noble gases in ultra low fields have the potential to resolve energies down to 10^{-25} eV
(but we are still far from that)

- Oscillating ALP fields generate two sidebands of the Larmor peak

- The two sidebands have the same amplitude and a well defined frequency relation
(how can we make more use of this?)

- ALPs of masses between 0.01 Hz … 10 Hz are detectable, if their coupling corresponds to a magnetic field between 0.1 fT … 100 fT, i.e. 3×10^{-9} GeV^{-1} … 3×10^{-6} GeV^{-1}

- Artefacts are identified by the presence of an additional peak at the modulation frequency „ν_{ALP}“

Acknowledgement

Thanks to:

DFG Priority Program SPP 1491

Hans-Helge Albrecht
Martin Burghoff
Isaak Fan
Wolfgang Kilian
Silvia Knappe-Grüneberg
Allard Schnabel
Frank Seifert
Detlef Stollfuß
Jens Voigt

MITP:

D. Budker
S. Rajendran
P. Graham